



Thermal behaviour of the nitrated AFm phase $\text{Ca}_4\text{Al}_2(\text{OH})_{12}(\text{NO}_3)_2 \cdot 4\text{H}_2\text{O}$ and structure determination of the intermediate hydrate $\text{Ca}_4\text{Al}_2(\text{OH})_{12}(\text{NO}_3)_2 \cdot 2\text{H}_2\text{O}$

G. Renaudin^a, J.-P. Rapin^a, B. Humbert^b, M. François^{a,*}

^aLaboratoire de Chimie du Solide Minéral, UMR 7555, Université Henri Poincaré, Nancy I, F-54506 Vandoeuvre les Nancy, France

^bLaboratoire de Chimie Physique pour l'Environnement, UMR 7564, Université Henri Poincaré, Nancy I, F-54506 Vandoeuvre les Nancy, France

Received 26 July 1999; accepted 1 December 1999

Abstract

The nitrated AFm phase $\text{Ca}_4\text{Al}_2(\text{OH})_{12}(\text{NO}_3)_2 \cdot 4\text{H}_2\text{O}$, which belongs to the layered double hydroxide family, is studied by thermogravimetric measurements and Raman microspectrometry as a function of temperature. Its structure at room temperature was determined previously. The existence of an intermediate hydrate around 70°C with composition $\text{Ca}_4\text{Al}_2(\text{OH})_{12}(\text{NO}_3)_2 \cdot 2\text{H}_2\text{O}$ was detected and its structure resolved by single crystal X-ray diffraction at that temperature. The structure at 70°C is described and has the rhombohedral space group $R\bar{3}c$ with cell parameters $a = 5.731(2)$ Å and $c = 48.32(1)$ Å and $Z = 3$. It can be considered as a pillared layer structure, because adjacent main layers $[\text{Ca}_2\text{Al}(\text{OH})_6]^+$ are bridged by nitrate groups. The remaining two water molecules are space filling only, and are not connected to the main layers. The structure exhibits dynamic disorder due to free rotation of nitrate groups around trigonal axes, in agreement with the Raman spectra. © 2000 Elsevier Science Ltd. All rights reserved.

Keywords: Crystal structure; Thermal analysis; Calcium aluminate cement; Nitrate

1. Introduction

$\text{Ca}_4\text{Al}_2(\text{OH})_{12}(\text{NO}_3)_2 \cdot 4\text{H}_2\text{O}$, or $3\text{CaO} \cdot \text{Al}_2\text{O}_3 \cdot \text{Ca}(\text{NO}_3)_2 \cdot 10\text{H}_2\text{O}$ in elementary oxide notation, is the AFm phase including nitrate groups as anionic species. Following the nomenclature usually employed in cement chemistry (e.g., monosulfoaluminate for $\text{Ca}_4\text{Al}_2(\text{OH})_{12} \cdot \text{SO}_4 \cdot 6\text{H}_2\text{O}$, monocarboaluminate for $\text{Ca}_4\text{Al}_2(\text{OH})_{12} \cdot \text{CO}_3 \cdot 5\text{H}_2\text{O}$, and hemicarboaluminate for $\text{Ca}_4\text{Al}_2(\text{OH})_{12} \cdot (\text{CO}_3)_{1/2} \cdot 6\text{H}_2\text{O}$), this compound can be named binitroaluminate. All these AFm phases belong to a wider family of compounds called layered double hydroxides. Our previous paper described the structure of binitroaluminate at room temperature [1]. It crystallizes in the trigonal space group $P\bar{3}c1$, with parameters $a = 5.7445(8)$ Å and $c = 17.235(5)$ Å. The structure consists of positively charged main layers $[\text{Ca}_2\text{Al}(\text{OH})_6]^+$ spaced 8.617(3) Å apart, where the Al^{3+} and Ca^{2+} cations are six and seven oxygen coordinated, respectively. The interlayer part $[\text{NO}_3, 2\text{H}_2\text{O}]^-$ is strongly disordered. First, it was shown that the nitrate group, which is linked to Ca atoms by an oxygen atom, is replaced statistically by a linked

water molecule, each two lattices. This disorder is considered to be static. Second, there exists also dynamic disorder due to free rotation of NO_3^- groups around the ternary axis of the structure.

Previous workers have studied the thermal behavior of binitroaluminate [2,3]. They indicated that structural changes as a function of temperature are probable, but have not been identified until now. In this paper, we study such structural changes. First, thermogravimetric measurements were used to follow the various steps of dehydration and denitration of this pure nitrate-AFm. Second, Raman spectrometry as a function of temperature was undertaken on a single crystal specimen to observe structural changes related to the dehydration reactions. The results showed at 70°C the existence of an intermediate binitroaluminate. Then, its structural determination based on X-ray single crystal diffraction data was performed at 70°C. This intermediate structure is compared with the room temperature structure.

2. Methods

2.1. Sample preparation

$\text{Ca}_4\text{Al}_2(\text{OH})_{12}(\text{NO}_3)_2 \cdot 4\text{H}_2\text{O}$ was prepared by hydrothermal synthesis in the same manner as in our previous work

* Corresponding author. Tel.: +33-3-83-91-24-99; fax: +33-3-83-91-21-66.

E-mail address: francois@lcsu.u-nancy.fr (M. François).

on AFm phases [4–6]. The starting powder was an intimate mixture of $\text{Ca}(\text{OH})_2$, $\text{Al}(\text{OH})_3$, and $\text{Ca}(\text{NO}_3)_2 \cdot 4\text{H}_2\text{O}$ in the mole ratio 3/2/1.

Phases present in the synthesized product were examined by powder X-ray diffraction (XRD) and the composition of the single crystals was checked using a scanning electron microscope (SEM) equipped with an energy-dispersive spectrometer (EDS).

2.2. Thermogravimetric analysis

Thermogravimetric analysis was carried out on about 100 mg of the sample, with a heating rate of $3^\circ\text{C}/\text{min}$ in a flux of dry nitrogen, from room temperature to 950°C . The apparatus comprised a self-regulating Chenevard-Joumier system T5TH-type oven (Adamel, Paris, France) connected to an electronic Ugine Eyraud system B70-type beam scale (Cetaram, Lyon, France).

2.3. Raman microspectrometry

The Raman spectrometer used in this work was a Jobin-Yvon T64000 device (Jobin-Yvon Spex, Paris, France) in triple subtractive mode with 1,800 grooves per mm gratings. The spectral resolution obtained with an excitation source at 514.50 nm is about 2.7 cm^{-1} . The Raman detector is a charged coupled device (CCD) camera cooled by liquid nitrogen to 140°K . The microscope coupled with the spectrometer allows us to record confocal Raman signals with a spatial lateral resolution better than $1\text{ }\mu\text{m}$ and an axial resolution better than $2\text{ }\mu\text{m}$ [7]. It is equipped with a motorized stage with a step of about 80 nm. We used a ($\times 50$) objective, with a numerical aperture of 0.55, at a working distance of 9 mm. This objective retains 98% of the initial polarization of the electrical field of the laser beam. The single crystals placed under the objective are either fixed at the extremity of a capillary positioned on a goniometer head or put in a heating cell with the laser beam perpendicular to the layers. The heating cell is closed with a glass that separates the heated sample from the objective to avoid damage to it. Moreover, the crystal is introduced in the crucible under a low relative pressure so as not to damage the microscope lens by conduction.

Temperatures indicated on Raman spectra obtained under weak pressure cannot be directly compared with the indicated temperatures on thermogravimetric experiments, which were realized at atmospheric pressure. The conditions of temperature (T_{Ram}) and pressure used during the Raman experiment and the estimated corresponding “thermogravimetric analysis (TGA) temperatures” (T_{TGA}) are indicated in Table 1 to facilitate comparison between TGA and Raman results.

2.4. Single-crystal XRD

An XRD study was performed on a single crystal mounted in an automatic CAD-4 Nonius diffractometer

Table 1

T_{Ram} and pressure for recording Raman spectra and the estimated corresponding temperature for (T_{TGA})

T_{Ram} and pressure	T_{TGA} ($^\circ\text{C}$)
25°C at P_{atm}	25
30°C at P_{atm}	30
40°C at 25 mbar	50
50°C at 10 mbar	70
60°C at 0.1 mbar	80

(Norius, Delft, The Netherlands). The data collection was performed at 70°C by using a low-cost heating device described elsewhere [8].

The single crystal used here was that used for determining the structure at room temperature [1]. The lattice parameters were refined with CAD-4 software [9] from 25 reflections in the θ range 3.5 to 11.5° with $\text{AgK}\alpha$ radiation ($\lambda = 0.56050\text{ }\text{\AA}$). Recording and refinement parameters are summarized in Table 2.

Reflections (1,129) were collected out to $\sin\theta/\lambda = 0.75\text{ }\text{\AA}^{-1}$, yielding 487 unique reflections ($R_{\text{int}} = 2.6\%$). Systematic absences ($-h + k + l \neq 3n$, $hkl: l \neq 3n$, $00l \neq 6n$) led to the possible space groups: $R\bar{3}c$ and $R3c$. Data reduction, in the $\bar{3}m$ Laue group, was performed using programs of Blessing's system [10]. An absorption correction was made using the SORTAV program [11] from Blessing's system, with minimum and maximum transmission factors of 0.75 and 0.95. Direct methods using the SIR97 program [12] assuming the centrosymmetric space group $R\bar{3}c$ located the Al, Ca, and O atoms belonging to the ordered main layers of the structure. Scattering factors used for structure factor calculation and transformed Fourier analysis were those of neutral atoms H, O, N, Al, and Ca and are internal to the program. The partial

Table 2

Crystal data and structure refinement for $\text{Ca}_4\text{Al}_2(\text{OH})_{12} \cdot (\text{NO}_3)_2 \cdot 2\text{H}_2\text{O}$ studied at 70°C

Compound	Binitroaluminate at 70°C $\text{Ca}_4\text{Al}_2(\text{OH})_{12} \cdot (\text{NO}_3)_2 \cdot 2\text{H}_2\text{O}$
Formula weight	560.41 $\text{g} \cdot \text{mol}^{-1}$
Temperature	333 (1) K
Wavelength	0.56050 \AA
Scan mode	ω -2 θ
Crystal system	Rhombohedral
Space group	$R\bar{3}c$
Unit cell dimensions	$a = 5.731(2)\text{ }\text{\AA}$ $c = 48.32(1)\text{ }\text{\AA}$
Volume	1324.8(7) \AA^3
Z/calculated density	3/2.031 $\text{g} \cdot \text{cm}^{-3}$
Absorption coefficient	0.702 mm^{-1}
F (000)	858
Crystal size	$0.320 \times 0.200 \times 0.075\text{ mm}^3$
Theta range for data collection	1.99° at 24.90°
Index ranges	$0 \leq h \leq 7, 0 \leq k \leq 7, 0 \leq l \leq 70$
Reflections collected/independent	1129/487 [$R_{\text{int}} = 2.6\%$]
Refinement method	Full-matrix least squares on F^2
Number of data/restraints/parameters	425 [$I > 2\sigma(I)$]/11/48
Goodness of fit on F_2	1.256
Final R indices [$I > 2\sigma(I)$]	$R1 = 0.0977, wR2 = 0.2443$
Largest difference peak and hole	$2.346\text{ e} \cdot \text{\AA}^{-3}$ and $-0.856\text{ e} \cdot \text{\AA}^{-3}$

solution was then refined by least square method using the SHELX97 program [13]. Atomic sites of the interlayer species (O atoms of the water molecules, N and O atoms of nitrate group) were more clearly positioned by Fourier difference maps. There are seven non-H-atomic positions in the structure, which were refined with anisotropic temperature factors. For the H-atoms the temperature factor was held at $1.20 U_{eq}$ of the corresponding O-atom. The H-atoms of the water molecules could not be localised. Restraints with standard deviation were used for the O-H distance ($0.95(1) \text{ \AA}$) and for the geometry of the nitrate groups, which were restrained to be flat with the three O-N-O angles equal to $120(1)^\circ$ and three identical but not fixed N-O distances. The z coordinates of N and O(n2) sites were fixed at $1/12$. Refinement of 48 parameters, using 11 restraints for 425 reflections with $I > 2\sigma(I)$, led to a final confidence factor of 0.0977.

3. Results and discussion

3.1. Thermogravimetric analysis

The thermogravimetric curves (integrated and derivative curves) are shown in Fig. 1. They were interpreted using information given by Ahmed et al. [2] on the thermal decomposition of this AFm phase. They allow a chemical analysis as a function of the temperature. Decomposition of the sample from room temperature (Tr) to 950°C occurs in four main steps marked by the maxima of the derivative curve. A first dehydration occurs at 70°C (point B), followed by a second dehydration at 110°C (point C) and, at higher temperatures, decomposition of the nitrate species: at 250°C nitrate is re-

duced to nitrite, and at 520°C the nitrite decomposes. At these relatively high temperatures dehydroxylation also occurs.

The relative weight loss (observed and calculated from chemical reactions) and the chemical composition as a function of the temperature are indicated in Table 3. Observed and calculated relative weight losses are in agreement, taking into account of the accuracy of the measurement, which is $\sim 5\%$. The complete thermal decomposition of the compound to a product of empirical composition $\text{Ca}_4\text{Al}_2\text{O}_7$ occurs at $1,300^\circ\text{C}$. The observed relative weight loss of 46.1% at that temperature corresponds to the thermal decomposition of the binitroaluminate of composition $\text{Ca}_4\text{Al}_2(\text{OH})_{12}(\text{NO}_3)_2 \cdot 4\text{H}_2\text{O}$. This result was expected and is in agreement with earlier XRD results [1]. From Tr to 100°C the relative weight loss is 8.8% and corresponds to the loss of three water molecules per formula unit. At 100°C , the compound has the composition $\text{Ca}_4\text{Al}_2(\text{OH})_{12}(\text{NO}_3)_2 \cdot \text{H}_2\text{O}$. At around $T_{\text{TGA}} = 70^\circ\text{C}$ (point B on Fig. 1), the water content is close to two water molecules per formula unit.

From 100 to 160°C , the weight loss is about 3% and corresponds to the final dehydration (loss of the fourth water molecule) leading to anhydrous $\text{Ca}_4\text{Al}_2(\text{OH})_{12}(\text{NO}_3)_2$. From 160 to $1,300^\circ\text{C}$, the relative weight loss of 35.2% (the various steps as a function of the temperature are detailed in the Table 3) is due to nitrate reduction, nitrite loss, and dehydroxylation as noted earlier.

3.2. Raman microspectrometry analysis

The observation of a two-stage dehydration process seems to indicate the existence of an intermediate hydrate

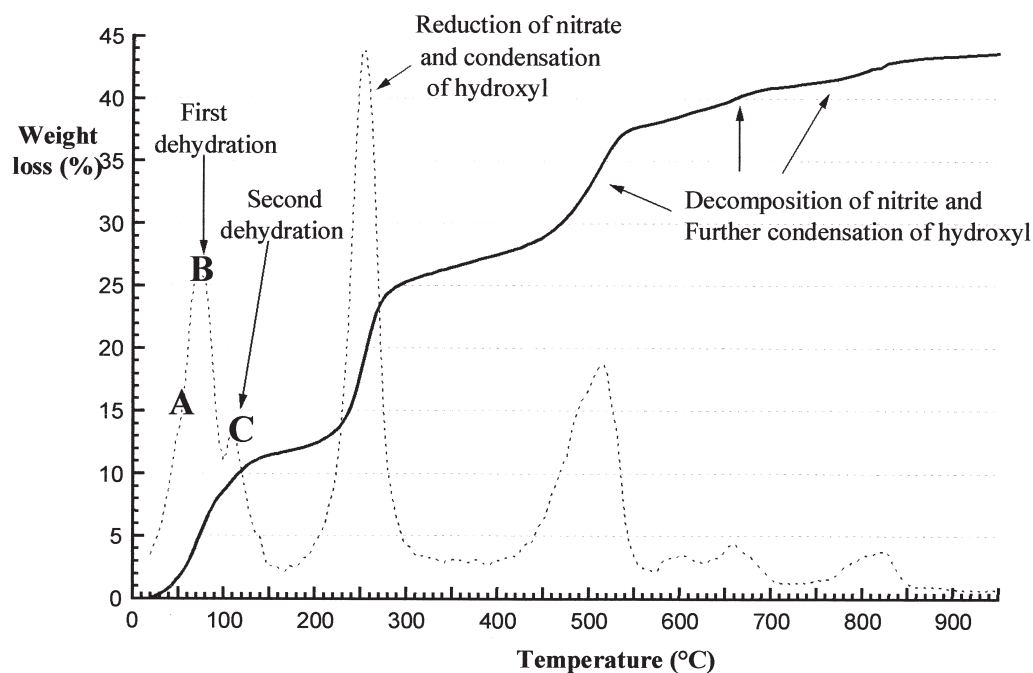


Fig. 1. TGA curve for a sample of binitroaluminate. The solid line represents the thermogravimetric curve and the dotted line represents the corresponding derivative curve.

Table 3

Thermal decomposition of binitroaluminate $\text{Ca}_4\text{Al}_2(\text{OH})_{12} \cdot (\text{NO}_3)_2 \cdot 4\text{H}_2\text{O}$

T_{TGA} (°C)	Observed weight losses (%)	Composition	Calculated weight losses (%)
25	0.0	$\text{Ca}_4\text{Al}_2(\text{OH})_{12} \cdot (\text{NO}_3)_2 \cdot 4\text{H}_2\text{O}$	0.0
100	8.6	$\text{Ca}_4\text{Al}_2(\text{OH})_{12} \cdot (\text{NO}_3)_2 \cdot \text{H}_2\text{O}$	8.8
160	11.6	$\text{Ca}_4\text{Al}_2(\text{OH})_{12} \cdot (\text{NO}_3)_2$	11.7
310	25.6	$\text{Ca}_4\text{Al}_2\text{O}_3(\text{OH})_6 \cdot (\text{NO}_2)_2$	25.7
425	28.1	$\text{Ca}_4\text{Al}_2\text{O}_4(\text{OH})_4 \cdot (\text{NO}_2)_2$	28.6
550	37.6	$\text{Ca}_4\text{Al}_2\text{O}_5(\text{OH})_4$	37.8
1,300	46.1	$\text{Ca}_4\text{Al}_2\text{O}_7$	46.9

with two water molecules per formula unit at $T_{\text{TGA}} = 70^\circ\text{C}$ (i.e., $\text{Ca}_4\text{Al}_2(\text{OH})_{12}(\text{NO}_3)_2 \cdot 2\text{H}_2\text{O}$). A Raman analysis has been performed on a single crystal under progressive heating to confirm the existence of this intermediate compound.

Fig. 2 reports Raman spectra with indications of the corresponding TGA temperatures (see also Table 1). Four series of spectra are displayed that correspond to the spectral ranges of (a) water stretching, (b) hydroxyl stretching, (c) the symmetric stretching mode A_1' of nitrate group, and (d) the degenerate in-plane bending mode, E' , of the nitrate group.

3.2.1. Water stretching modes

At room temperature, two large bands of vibration are shown near $3,270$ and $3,420\text{ cm}^{-1}$ and indicate two types of H-bonds of water molecules present in binitroaluminate. The broad band centered at $3,420\text{ cm}^{-1}$ with a full width at half height (FWHH) of 105 cm^{-1} has a profile similar to those obtained for water molecules in the liquid phase. The other component at $3,270\text{ cm}^{-1}$ corresponds to water molecules strongly bonded to an acceptor of a H-bond or a Fermi resonance. This is in good accordance with the structure determination [1], which makes clear the existence of water molecules directly bonded to the main layer and weakly bonded water molecules in the midway parts of the interlayers. Raman spectra obtained at $T_{\text{TGA}} = 30^\circ\text{C}$ ($T_{\text{Ram}} = 30^\circ\text{C}$ and atmospheric pressure) and at $T_{\text{TGA}} = 50^\circ\text{C}$ ($T_{\text{Ram}} = 40^\circ\text{C}$ and $P = 25\text{ mbar}$) have similar profiles with a weakening of the broad band at $3,270\text{ cm}^{-1}$ and a continuous shift from $3,420$ to $3,435\text{ cm}^{-1}$ of the other component. At $T_{\text{TGA}} = 70^\circ\text{C}$ ($T_{\text{Ram}} = 50^\circ\text{C}$ and $P = 10\text{ mbar}$) the profile has changed: a weak broad component is displayed at about $3,250\text{ cm}^{-1}$ while the other component is narrower (FWHH = 37 cm^{-1}) and shifts to a higher wave number ($3,480\text{ cm}^{-1}$). Finally, at $T_{\text{TGA}} = 80^\circ\text{C}$ ($T_{\text{Ram}} = 60^\circ\text{C}$ and $P = 10^{-1}\text{ mbar}$) only a weak signal, very broad, is observed at about $3,300\text{ cm}^{-1}$. This last component disappears at a temperature higher than 100°C (not shown here), indicating the absence of water molecules and formation of anhydrous $\text{Ca}_4\text{Al}_2(\text{OH})_{12}(\text{NO}_3)_2$, obtained in thermogravimetric experiments at temperatures higher than 140°C . This series of spectra relevant to vibration of water molecules shows clearly that an intermediate hydrate is present at $T_{\text{TGA}} =$

70°C (or at $T_{\text{Ram}} = 50^\circ\text{C}$ and $P = 10\text{ mbar}$), which corresponds to point B on TGA curves (Fig. 1).

3.2.2. Hydroxyl stretching

The second series of spectra relating to hydroxyl stretching also shows a different type of spectrum at $T_{\text{TGA}} = 70^\circ\text{C}$ ($T_{\text{Ram}} = 50^\circ\text{C}$ and $P = 10\text{ mbar}$), corresponding to a different hydrogen bonding network. In this spectral range from $3,550$ to $3,750\text{ cm}^{-1}$, the Raman spectrum at room temperature is composed of an intense band at $3,670$ (FWHH = 24 cm^{-1}) with a shoulder at $3,642\text{ cm}^{-1}$. The value of FWHH is higher than those observed for monocarboaluminate, for instance, for which the value is 5 cm^{-1} . This fact is an indication of a dynamic disorder as previously indicated in the structural determination of binitroaluminate at room temperature [1]. Free rotation of the nitrate groups and weakly bonded water molecules around the trigonal axis (of the space group $R\bar{3}c$) generates a continuous reorganization of the hydrogen bonding network. In contrast, the hydroxyl stretching bands in Raman spectra from the ordered $\text{O-C}_4\text{ACH}_{11}$ and disordered $\text{D-C}_4\text{ACH}_{11}$ forms of monocarboaluminate display a narrowness of bands due to well-defined hydrogen bonds. The dihydrate, $\text{Ca}_4\text{Al}_2(\text{OH})_{12}(\text{NO}_3)_2 \cdot 2\text{H}_2\text{O}$ also exhibits dynamic disorder in the interlayer part of its structure since the broad components at $3,655$ and $3,683\text{ cm}^{-1}$ observed at $T_{\text{TGA}} = 70^\circ\text{C}$ (at $T_{\text{Ram}} = 50^\circ\text{C}$ and $P = 10\text{ mbar}$) are characterized respectively by FWHH values of 48 and 20 cm^{-1} . The shift of the components from $3,642$ to $3,655\text{ cm}^{-1}$ and from $3,670$ to $3,683\text{ cm}^{-1}$ shows clearly that the H bonds of the hydroxyls as H-donors are weaker.

3.2.3. Nitrate modes of vibration

The observations on the nitrate vibration modes confirm that a change occurs when the crystal is heated at $T_{\text{TGA}} = 70^\circ\text{C}$ ($T_{\text{Ram}} = 50^\circ\text{C}$ and $P = 10\text{ mbar}$). The symmetric stretching mode ν_2 (A_1' mode) shifts from $1,059\text{ cm}^{-1}$ (FWHH = 8 cm^{-1}) at room temperature to $1,070\text{ cm}^{-1}$ (FWHH = 11 cm^{-1}) at $T_{\text{TGA}} = 70^\circ\text{C}$. This shift to higher wave numbers indicates, as the case of hydroxyl groups, a decrease of H bonds with nitrate group. At temperatures higher than 70°C , this mode shifts to $1,055\text{ cm}^{-1}$ with an FWHH value of 4 cm^{-1} . This last fact must be correlated with reorientation of nitrate group, which became parallel to the layers [2], the main consequence of this being the formation of new H bonds. Thus, the dihydrate would be interpreted as having the strongest N-O bonds, compared to the compound at room temperature and at 80°C (that is, the weakest interactions between the oxygen atoms and the rigid layers of the structure).

The degenerated E' mode, ν_4 in-plane bending, at about 720 cm^{-1} , which splits slightly into two bands at about 717 and at 723 cm^{-1} at room temperature [6], splits clearly into two components separated by 12 cm^{-1} at $T_{\text{TGA}} = 70^\circ\text{C}$ (at $T_{\text{Ram}} = 50^\circ\text{C}$ and $P = 10\text{ mbar}$). At $T_{\text{TGA}} = 80^\circ\text{C}$ (at $T_{\text{Ram}} = 60^\circ\text{C}$ and $P = 10^{-1}\text{ mbar}$), the splitting disappears and the only component preserved is at about 702 cm^{-1} with an FWHH value of about 7 cm^{-1} . This last observation allows

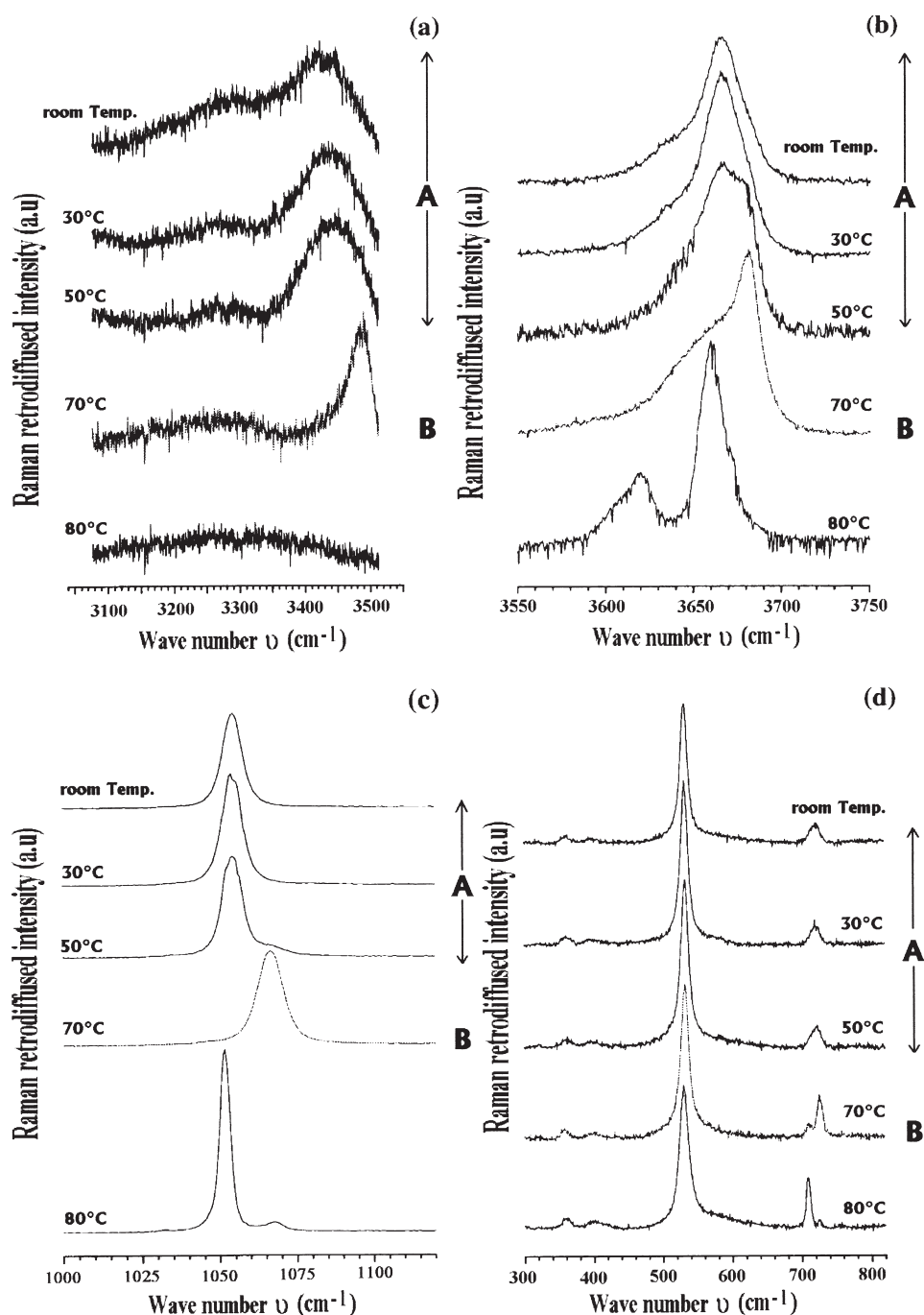


Fig. 2. Raman microspectrometry analysis: (a) stretching vibrations of water molecules, (b) hydroxyl stretching, (c) nitrate symmetric stretching mode A_1' , and (d) nitrate degenerated E' mode at about 730 cm^{-1} (antisymmetric stretching and planar angular deformation). The intense band at 540 cm^{-1} corresponds to aluminate vibration.

us to conclude that at $T_{\text{TGA}} = 70^\circ\text{C}$ (at $T_{\text{Ram}} = 50^\circ\text{C}$ and $P = 10\text{ mbar}$) two oxygen atoms of the nitrate group are bonded with two different Ca atom, whereas at room temperature only one oxygen atom of the nitrate group makes such a bond. XRD results confirmed this modification in the structure (this is described in the structural study of dihydrate).

In summary, interpretations of these four series of spectra prove the existence of a definite intermediate hydrate at $T_{\text{TGA}} = 70^\circ\text{C}$ and that compared with the higher hydrate, the water

molecules in it are only weakly bonded and exhibit a dynamic disorder. The environment of nitrate groups is modified and the hydrogen bonding is weaker than in the higher hydrate.

3.3. Structural study of $\text{Ca}_4\text{Al}_2(\text{OH})_{12}(\text{NO}_3)_2 \cdot 2\text{H}_2\text{O}$

3.3.1. Refinement results

Atomic parameters are summarised in Tables 4 and 5 and selected interatomic distances in Table 6. The refined occu-

Table 4

Atomic coordinates and equivalent isotropic temperature factor ($\text{\AA}^2 \times 10^3$) for $\text{Ca}_4\text{Al}_2(\text{OH})_{12} \cdot (\text{NO}_3)_2 \cdot 2\text{H}_2\text{O}$ studied at 70°C

Groups	Atoms	Sites	X	Y	Z	U_{eq}^a ($\text{\AA}^2 \times 10^3$)	Occupancy
Hydroxyl	Al	6(b)	0	0	0	16(1)	1
	Ca	12(c)	2/3	1/3	0.0113(1)	19(1)	1
	O	36(f)	0.0556(7)	0.3054(6)	0.0209(1)	19(1)	1
	H	36(f)	0.07(2)	0.29(2)	0.0402(5)	22(–)	1
Nitrate	O(n1)	12(c)	2/3	1/3	0.0614(2)	75(5)	1
	O(n2)	36(f)	0.53(3)	0.57(2)	1/12(–)	320(14)	1/6
	N	36(f)	0.622(9)	0.411(8)	1/12(–)	110(3)	1/6
Water	O(w)	36(f)	0.11(3)	0.86(3)	0.0880(8)	340(15)	0.17(3)

^a U_{eq} is defined as one third of the trace of the orthogonalized U_{ij} tensor.

pancy factor of 0.17(3) for the O(w) site shows that there are two water molecules per formula unit. Thus, the intermediate hydrate measured here, at 70°C in normal atmosphere, has a composition close to $\text{Ca}_4\text{Al}_2(\text{OH})_{12}(\text{NO}_3)_2 \cdot 2\text{H}_2\text{O}$. Its structure is represented in Fig. 3, with that of $\text{Ca}_4\text{Al}_2(\text{OH})_{12}(\text{NO}_3)_2 \cdot 4\text{H}_2\text{O}$ for comparison. The main $[\text{Ca}_2\text{Al}(\text{OH})_6]^+$ layers are those usually encountered in AFm phases with Al-atoms in a regular octahedral hydroxyl coordination [six Al-O distances of 1.902(3) Å] and the coordination number of the Ca-atoms is augmented to seven, with Ca-O distances of 2.356(3) to 2.434(4) Å. On heating from Tr to 70°C, the main layers undergo a sideways translatory motion and the interlayer distance decreases from 8.62 to 8.05 Å. In the completely hydrated compound, the main layers are stacked so as to space out as well as possible the water molecules linked to a layer (through Ca atom) and to the adjacent one [1]. In the dihydrate at 70°C, the seventh neighbours of the Ca-atoms are all O atoms of nitrate groups. An important feature of the dihydrate is thus that the main layers are bridged by NO_3^- groups, forming a pillar structure. There are no strongly bonded water molecules in this lower hydrate. The water present at 70°C is situated midway in the interlayer part of the structure, and is only weakly bonded by hydrogen bonds.

As in the room temperature structure [1], the NO_3^- groups are dynamically disordered. This results from free rotation movement of NO_3^- around the trigonal axis [i.e., the O(n1) \cdots O(n1) direction]. It is modelled by a shift from special position 12c (2/3, 1/3, z) to a general position for the

central N atom of the nitrate group and by relatively high temperature factors for these atoms. It is worth noticing that the N-O distances of 1.22(1) Å in $\text{Ca}_4\text{Al}_2(\text{OH})_{12}(\text{NO}_3)_2 \cdot 2\text{H}_2\text{O}$ are slightly lower than those of 1.24(1) Å determined in $\text{Ca}_4\text{Al}_2(\text{OH})_{12}(\text{NO}_3)_2 \cdot 4\text{H}_2\text{O}$.

3.3.2. Comparison with Raman and TGA results

The Raman spectra at $T_{\text{TGA}} = 70^\circ\text{C}$ (point B) are consistent with the structural model found by XRD. The main differences concerning the vibration of water molecules, hydroxyl and nitrate groups when going from $\text{Ca}_4\text{Al}_2(\text{OH})_{12}(\text{NO}_3)_2 \cdot 4\text{H}_2\text{O}$ to $\text{Ca}_4\text{Al}_2(\text{OH})_{12}(\text{NO}_3)_2 \cdot 2\text{H}_2\text{O}$ are discussed next.

There remains only free water molecules, which are better organised (shift to higher wave number and lower FWHH, see Fig. 2a). A decrease in the number and strength of hydrogen bonds between H of hydroxyl groups and the interlayer species (i.e., water molecules and nitrate groups) due to loss of water (shift to higher wave number and lower FWHH, see Fig. 2b) is observed.

An important change occurs in the environment of the nitrate groups (shift to higher wave number, see Fig. 2c), which bridges adjacent main layers. The symmetric vibration of the nitrate group at $1,070\text{ cm}^{-1}$ in $\text{Ca}_4\text{Al}_2(\text{OH})_{12}(\text{NO}_3)_2 \cdot 2\text{H}_2\text{O}$ indicates stronger N-O bonds, in agreement with the shortened N-O distances. The point A on the TGA diagram corresponds to a mixture of the tetrahydrated and the dihydrated compound, point B corresponds to the dihydrated compound, and point C corresponds to the compound with less than one water molecule per formula unit.

Table 5

Anisotropic temperature factor ($\text{\AA}^2 \times 10^3$) for $\text{Ca}_4\text{Al}_2(\text{OH})_{12} \cdot (\text{NO}_3)_2 \cdot 2\text{H}_2\text{O}$ studied at 70°C

Atoms	U_{11}	U_{22}	U_{33}	U_{23}	U_{13}	U_{12}
Al	7(1)	7(1)	33(2)	0	0	3(1)
Ca	10(1)	10(1)	36(1)	0	0	5(1)
O	12(2)	7(1)	37(2)	–3(1)	–2(1)	4(1)
O(n1)	98(8)	98(8)	28(4)	0	0	49(4)
O(n2)	500(300)	600(300)	170(70)	–210(140)	–220(140)	500(300)
N	220(80)	80(60)	41(14)	–20(60)	–20(60)	100(60)
O(w)	300(180)	230(120)	20(30)	–10(40)	–10(40)	–210(120)

The anisotropic displacement factor exponent takes the form: $-2\pi^2 [h^2 a^{*2} U_{11} + \dots + 2 h k a^* b^* U_{12}]$.

Table 6

Selected inter atomic distances Ca-O, Al-O, and N-O for $\text{Ca}_4\text{Al}_2(\text{OH})_{12} \cdot (\text{NO}_3)_2 \cdot 2\text{H}_2\text{O}$ studied at 70°C

Atoms	Distance (Å)	Atoms	Distance (Å)
Al-O	1.902(3)	Ca-O#6	2.356(3)
Al-O#1	1.902(3)	Ca-O#3	2.356(3)
Al-O#2	1.902(3)	Ca-O#7	2.356(3)
Al-O#3	1.902(3)	Ca-O(n1)	2.415(7)
Al-O#4	1.902(3)	Ca-O#8	2.434(4)
Al-O#5	1.902(3)	Ca-O#9	2.434(4)
		Ca-O#4	2.434(4)
N-O(n1)	1.22(1)	N-O(n2)	1.22(1)
N-O(n1)#10	1.22(1)		

Symmetry operators generating equivalent positions: #1 $-x, -y, -z$; #2 $x - y, x, -z$; #3 $-x + y, -x, z$; #4 $y, -x + y, -z$; #5 $-y, x - y, z$; #6 $x + 1, y, z$; #7 $-y + 1, x - y + 1, z$; #8 $x - y + 1, x, -z$; #9 $-x + 1, -y + 1, -z$; #10 $y + 1/3, x - 1/3, -z + 1/6$.

At 160°C the completely dehydrated one, $\text{Ca}_4\text{Al}_2(\text{OH})_{12}(\text{NO}_3)_2$ (not studied here), probably has a different structure. Indeed, the Raman spectra of Fig. 2d indicate that the orientation of the nitrate group, perpendicular to the layer from Tr to $T_{\text{TGA}} = 70^\circ\text{C}$, becomes parallel above that temperature. This was suggested by XRD evidence [2]. Study of the structure at a temperature slightly above 80°C is in progress.

Another point of interest is the reversibility of the suc-

$\text{Ca}_4\text{Al}_2(\text{OH})_{12} \cdot (\text{NO}_3)_2 \cdot 2\text{H}_2\text{O}$

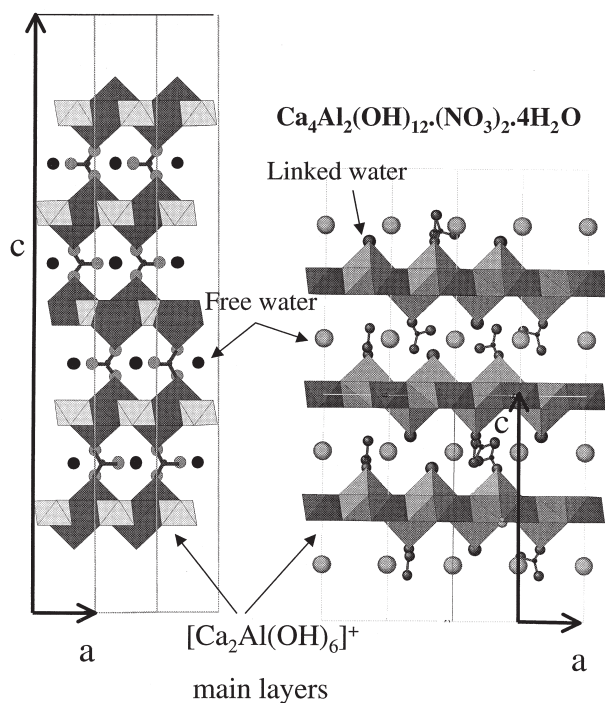


Fig. 3. Projection on (010) of (a) dihydrated and (b) tetrahydrated binitrioaluminate. The main layers are drawn showing the AlO_6 and CaO_7 polyhedra. The inter layer parts of the structures have been ordered for clarity; in (a) the NO_3^- groups are simply represented by two orientations and H_2O molecules are placed on the 12c special position.

cessive dehydration. Raman and XRD results (not presented here) confirms a previous observation [2] that the product obtained around 100°C and of composition close to $\text{Ca}_4\text{Al}_2(\text{OH})_{12}(\text{NO}_3)_2$ absorbs water present in the atmosphere at room temperature, giving the fully hydrated compound $\text{Ca}_4\text{Al}_2(\text{OH})_{12}(\text{NO}_3)_2 \cdot 4\text{H}_2\text{O}$.

4. Conclusions

It has been shown that the crystal structures of the higher and lower hydrate $\text{Ca}_4\text{Al}_2(\text{OH})_{12}(\text{NO}_3)_2 \cdot 4\text{H}_2\text{O}$ and $\text{Ca}_4\text{Al}_2(\text{OH})_{12}(\text{NO}_3)_2 \cdot 2\text{H}_2\text{O}$, respectively, are significantly different. The first has a distinct layer structure (2D), while the second contains similar layers that, however, are bonded together by nitrate groups, giving a pillared layer structure. The only water molecules in the dihydrate are weakly bonded through H bonds in the interlayer. Interpretation of the Raman spectra in the temperature range 25 to 70°C is in agreement with the structural description given for the phase at room temperature and 70°C.

Structural changes also occur during the loss of the two remaining water molecules when heating from 70 to 160°C. We suspect that the nitrate groups become parallel to the main layers of the structure at 80°C. A structural study of the compound at that temperature range is in progress.

It has also been shown that the full dehydration from $\text{Ca}_4\text{Al}_2(\text{OH})_{12}(\text{NO}_3)_2 \cdot 4\text{H}_2\text{O}$ to $\text{Ca}_4\text{Al}_2(\text{OH})_{12}(\text{NO}_3)_2$ is reversible.

Acknowledgments

The authors are grateful to the Service Commun de Diffractométrie Automatique of the University Henri Poincaré, Nancy, and Alain Rouillier from the Laboratoire d'Expérimentation Haute Température—Basse Pression (CRPG), Nancy, for the autoclave operations.

References

- [1] G. Renaudin, M. François, The lamellar double-hydroxide (LDH) compound with composition $3\text{CaO} \cdot \text{Al}_2\text{O}_3 \cdot \text{Ca}(\text{NO}_3)_2 \cdot 10\text{H}_2\text{O}$, *Acta Cryst C* 55 (1999) 835–838.
- [2] S.J. Ahmed, L.S. Dent Glasser, H.F.W. Taylor, Crystal structures and reactions of C_4AH_{12} and derivated basic salts, 5th Int. Symp. on the Chem. of Cement, Supp. Paper II-77, Tokyo, 1968.
- [3] H.J. Kuzel, Über die hydrastufen der hydroxysalze $3\text{CaO} \cdot \text{Me}_2\text{O}_3 \cdot \text{CaCl}_2 \cdot n\text{H}_2\text{O}$ und $3\text{CaO} \cdot \text{Me}_2\text{O}_3 \cdot \text{Ca}(\text{NO}_3)_2 \cdot n\text{H}_2\text{O}$, *Neues Jahr Miner Monats* (1970) 363–373.
- [4] M. François, G. Renaudin, O. Evrard, A cementitious compound with composition $3\text{CaO} \cdot \text{Al}_2\text{O}_3 \cdot \text{CaCO}_3 \cdot 11\text{H}_2\text{O}$, *Acta Cryst C* 54 (1998) 1214–1217.
- [5] G. Renaudin, M. François, O. Evrard, Order and disorder in the lamellar hydrated tetracalcium monocarboaluminate compound, *Cem Concr Res* 29 (1999) 63–69.
- [6] G. Renaudin, I. Etude d'un hydroxyde simple d'aluminium: La bayérite, II. Etude d'une famille d'hydroxydes doubles lamellaires d'alu-

- minium et de calcium: Les phases AFm (aluminate tetracalciques hydratés), Thesis, University Henri Poincaré, Nancy I, France, 1998.
- [7] J. Grausem, Analyse du champ proche optique inélastique. Réalisation et application d'une nanosonde pour la spectrométrie Raman, Thesis, University Henri Poincaré, Nancy I, France, 1998.
- [8] O. Crottaz, F. Kubel, H. Schmid, High temperature single crystal X-ray diffraction: Structure of cubic manganese iodine and manganese bromine boracite, *J Solid State Chem* 120 (1) (1995) 60–65.
- [9] Enraf-Nonius, CAD-4 Software Version 5.0, Enraf-Nonius, Delft, The Netherlands, 1989.
- [10] R.H. Blessing, Data reduction and error analysis for accurate single crystal diffraction intensities, *Crystallogr Rev* 1 (1987) 3–58.
- [11] R.H. Blessing, An empirical correction for absorption anisotropy, *Acta Cryst A* 51 (1995) 33–38.
- [12] A. Altomare, M.C. Burla, M. Camalli, G. Cascarano, C. Giacovazzo, A. Guagliardi, G. Polidori, SIR97 program: A new tool for crystal structure determination, *J Appl Cryst* 32 (1999) 115–119.
- [13] G.M. Sheldrick, SHELX97, Program for the refinement of crystal structure, University of Göttingen, Germany, 1997.